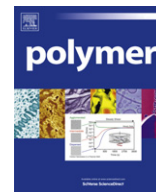


Contents lists available at [SciVerse ScienceDirect](http://www.sciencedirect.com)

Polymer

journal homepage: www.elsevier.com/locate/polymer

Photophysics of polyaniline: Sequence-length distribution dependence of photoluminescence quenching as studied by fluorescence measurements and Monte Carlo simulations

P. Soledad Antonel, Edgar Völker, Fernando V. Molina*

Instituto de Química Física de Materiales, Ambiente y Energía (INQUIMAE), Facultad de Ciencias Exactas y Naturales, Universidad de Buenos Aires, Buenos Aires, Argentina

ARTICLE INFO

Article history:

Received 23 February 2012

Received in revised form

17 April 2012

Accepted 22 April 2012

Available online xxx

Keywords:

Conducting polymers

Terpolymerization

Microstructure

ABSTRACT

The dependence of the fluorescence quenching of electropolymerized poly(aniline-co-*m*-chloroaniline) with polymer composition has been investigated. Fluorescence emission in polyaniline is quenched when the polymer is oxidized (brought to emeraldine state); the copolymers exhibit decreasing quenching as chloroaniline contents increases. Quenching shows a strong decrease in the presence of 0.1% *m*-chloroaniline monomers in the feed. The presence of dichloroaniline units in the copolymer was confirmed by XPS measurements and a terpolymerization reaction scheme was developed, obtaining the kinetic parameters. By Monte Carlo simulation the sequence length distributions for different compositions were obtained and compared; it was found that quenching, for low aniline contents, requires aniline sequences of at least three units. The strong decrease in quenching at low *m*-chloroaniline contents is attributed to a double effect: breaking of conjugation in the emeraldine form by the presence of the chlorinated unit, and a disruption of the close chain packing in the crystalline domains, preventing state delocalization and thus efficient quenching.

© 2012 Elsevier Ltd. All rights reserved.

1. Introduction

Aryl amine conducting polymers, mainly polyaniline (PANI), are very well known due to their interesting chemical, mechanical and optical properties (such as electrochromism, fluorescence, etc.) leading to a high number of proposed applications [1,2]. PANI and similar polymers show photoluminescence in their reduced state, which is quenched when the polymer is oxidized [3–8].

The redox switching of PANI and similar polymers is usually interpreted in terms of two redox states, the reduced leucoemeraldine and oxidized emeraldine, the conversion between them being a two-electron reaction [1,9]. The emeraldine state shows quenching of the PANI photoluminescence, with a gradual change in emission intensity for films on electrodes under potentiostatic control when the polymer is gradually oxidized [3,5,6]. From a structural point of view, it has been shown [10–13] that PANI films are actually composed of small, crystalline, conductive domains where the polymer chains are in close contact; these

domains are separated by amorphous low conductivity regions. In a previous study [6], the photophysical behavior of PANI films as a function of applied potential was studied. A decrease in emission intensity was observed as the polymer film is oxidized, leaving a small but finite emission when the polymer is in the emeraldine state. This behavior was consistent with a film structure composed of crystalline domains separated by amorphous regions, the emission being efficiently quenched in or near those ordered domains.

Due mainly to practical reasons, copolymers of aniline (Ani) with other aryl amines have been investigated [14–21]. Among these copolymers, chloroanilines have been regarded as attractive candidates for copolymerization with Ani due to the enhanced solubility in common solvents. Díaz et al. [22] chemically synthesized and characterized copolymers of aniline and dichloroanilines at several monomer ratios. Li et al. [23] synthesized by chemical oxidation and characterized systematically copolymers of aniline with *o*- and *m*-chloroaniline (mCIA). These authors reported that, in their working conditions (oxidant:monomer ratio of 0.5:1), the poly(*m*-chloroaniline) homopolymer (PmCIA) could not be obtained. Waware and Umare [24] synthesized by chemical oxidation Ani-mCIA copolymers in all the range, including PmCIA using an oxidant:monomer ratio of 1:1. Recently [8], the Ani-mCIA copolymerization in variable ratios was performed by chemical oxidation, determining the resulting copolymer composition by

* Corresponding author. Instituto de Química Física de Materiales, Ambiente y Energía (INQUIMAE), Facultad de Ciencias Exactas y Naturales, Universidad de Buenos Aires, Ciudad Universitaria, Pabellón II, piso 1, C1428EHA Buenos Aires, Argentina. Tel.: +54 11 4576 3378/80x230; fax: +54 11 45763341.

E-mail address: fmolina@qi.fcen.uba.ar (F.V. Molina).

elemental analysis and X-ray photoelectron spectroscopy (XPS). The results show the incorporation of additional Cl substituents in the polymer backbone for high mCIA:Ani ratios, leading to a dichloroaniline (dCIA) homopolymer in the absence of Ani. UV–Vis spectra were recorded, and comparison with PM3-ZINDO/S spectra calculations suggested that the Cl substituents stabilize spinless semiquinone structures in the polymer chain. Photoluminescence spectra were recorded and analyzed, but the lack of control of the oxidation state prevented detailed analysis. The addition of chlorine was attributed to chlorination of mCIA due to the lower reaction rate in high mCIA:Ani ratio.

The aim of this work is to study the photophysical behavior of electrosynthesized aniline-co-*m*-chloroaniline polymer films, as a function of applied potential, and to correlate it to the polymer microstructure. To this end, copolymer films were galvanostatically synthesized at different feed compositions, analyzed by XPS, their photoluminescence spectra recorded as a function of applied electrode potential, and the results related to the polymer microstructure as found by Monte Carlo simulations of the polymerization kinetics. The Monte Carlo method has been extensively applied in polymer science [25–29], particularly to copolymerization problems [30–34], where it has been shown to be a powerful tool to elucidate problems such as copolymer composition and sequence length distributions.

2. Experimental

2.1. Chemicals and materials

AR grade chemicals and high purity water from a MilliQ system were employed. Aniline (Fluka) was distilled under reduced pressure and reducing conditions shortly before use and *m*-chloroaniline (Fluka) was used as received.

A Teq-03 (S. Sobral, Buenos Aires, Argentina) potentiostat under computer control was employed in all the experiments. Both the electropolymerization and the spectroscopic experiments were conducted in a specially constructed cell, allowing to perform electrochemical processes with simultaneous fluorescence or absorbance measurements [5]. It has a rectangular shape (6 cm × 9 cm, 5 cm tall, wall thickness 0.50 cm), made of high molecular weight polyethylene. The working electrode was a rectangular glass covered with a fluorine-doped tin oxide (FTO) conducting layer, with a surface area in contact with solution of about 1 cm², and was mounted on a rotatory holder in order to adjust the incidence angle. The FTO electrode had a resistance of 21–25 Ω/□. A platinum auxiliary electrode was placed in a compartment separated by a porous glass, to avoid contamination of the working electrode solution with CE products; this compartment was filled with the same solution as the main one. The reference electrode was a reversible hydrogen one (RHE) in the same solution as the working electrode. All potentials are referred to this electrode.

2.2. Electropolymerization

The copolymerization of mCIA and Ani in variable ratios was performed by galvanostatic oxidation in 2 M HCl medium. Other electrochemical methods (cyclic voltammetry and potentiostatic oxidation) were not employed due to the low polymerization rate observed for polymerization solutions (feed) rich in mCIA [8,35]. All solutions used had a total monomer concentration of 0.1 M in 2 M HCl, but with different Ani and mCIA mole fractions, f_1 and f_2 respectively, in order to obtain copolymers of different composition. The electrosynthesis conditions in all cases were:

- 1) 10 min at a constant current of 3 mA cm⁻².
- 2) Rinsing of the working electrode (FTO) with MilliQ water
- 3) 5 min at 3 mA cm⁻².
- 4) Repetition of item 2.

With these conditions, thin copolymer films were obtained. To obtain the polymers in base form, the FTO glasses were soaked in ammonia solution for 1 h and afterward thoroughly rinsed with MilliQ water.

2.3. XPS measurements

XPS measurements were performed using a Specs Sage 150 spectrometer equipped with a dual anode Mg/Al X-ray source and a hemispherical electron energy analyzer. Spectra were acquired using a monochromatic MgK_α (1253.6 eV) source with a 90° detection angle. Quoted binding energies are referred to the adventitious C 1s emission at 285 eV, in order to compensate for charging effects. Measurements were made directly by placing the FTO electrode covered with each copolymer in the oxidized-base form into the spectrometer.

2.4. Cyclic voltammetry

The polymer films were electrochemically characterized by cyclic voltammetry in the potential region of the first anodic peak, to avoid degradation due to oxidation to pernigraniline [9]. The FTO glasses covered with the polymer films were thoroughly rinsed with MilliQ water to remove the polymerization solution and placed in a monomer free 2 M HCl solution, cycled at 50 mV s⁻¹ until a stationary voltammogram (usually 3–5 cycles) was obtained, and the last cycle was recorded.

2.5. Fluorescence of copolymer films as a function of potential

The resulting copolymers were characterized by fluorescence emission spectroscopy at different electrode potentials between 0.1 and 0.8 V. At each applied potential, the spectrum was recorded when the current (absolute value) was below 1 μA cm⁻². These measurements were also done in 2 M HCl.

The fluorometric measurements were performed using a PTI Quantmaster stationary spectrofluorometer with the same cell described previously [5]. The incidence angle was set at 30°, to avoid direct reflection of the excitation beam into the photomultiplier. The excitation wavelength, λ_0 , was set at 330 nm and the emission range, λ_e , was 350–600 nm.

3. Results

3.1. Copolymer electrosynthesis and characterization

Copolymers were synthesized by galvanostatic electropolymerization, as others methods (such as cyclic voltammetry or fixed potential) did not yield products for high values of f_2 or pure mCIA. It was observed that during the galvanostatic experiments the electrode potential reached values in excess of 2 V, and gas evolution was observed, thus Cl₂ production should take place. The composition was investigated by XPS measurements. From the XPS spectra the areas under the C 1s, N 1s and Cl 2p peaks were computed and, using appropriate instrumental factors, the ratios Cl/N (F_{Cl}), which is the average number of chlorine atoms per monomer unit, and C/N were obtained. In all the measurements, the ratio C/N was within 6.0 ± 0.3 as expected. Fig. 1 (closed circles) shows the F_{Cl} values obtained as a function of the Ani mole fraction

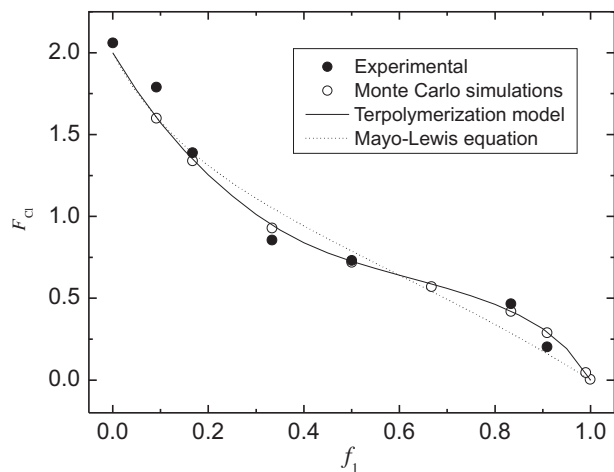


Fig. 1. Cl/N ratio in the copolymer films as a function of Anisole mole fraction in the feed. Closed symbols: XPS experimental results; open symbols: Monte Carlo simulation results; dotted line: best fit to the Mayo–Lewis equation (Equation (3), with $r_1 = 0.35$, $r_2 = 1.08$); continuous line: fit to the terpolymerization model. The simulation and fitting results are presented and discussed in Section 4.

in the feed, f_1 . The other symbols and curves, which represent model fittings, will be addressed in the Discussion section.

The results clearly show the incorporation of additional Cl substituents in the polymer chain, as a mCIA homopolymer will have $F_{Cl} = 1.0$. This has been observed previously [8] for chemically polymerized Anisole-mCIA copolymers; in the case of a mCIA feed free of Anisole, the accumulation of oxidant (ammonium persulfate) causes the oxidation of Cl^- to Cl_2 , chlorine reacts with mCIA giving dichloroaniline (dCIA), which polymerizes producing a dCIA homopolymer, as evidenced by the F_{Cl} value and spectroscopical studies [8]; it has also been observed that slow Anisole polymerization in high HCl concentrations leads to chlorine incorporation into the product [36]. In the present case, it is clear that a similar process is taking place: Cl^- is oxidized at the electrode surface with the same final result. Attempts to polymerize mCIA in the absence of Cl^- anions using other strongly acid media such as $HClO_4$ or H_2SO_4 did not yield any polymer, even under very strong conditions, thus confirming that monomer chlorination is required to obtain a polymer from mCIA. The alternative possibility, that is chlorination of the polymer product, is discarded as in the previous study [8], based on the following facts:

- 1) Anisole polymerization in the same conditions yields PANI homopolymer with no Cl in its composition, also observed for chemical polymerization [8].
- 2) The mCIA monomer does not homopolymerize at low oxidant concentrations [23] in HCl media, nor polymerizes in other media (such as H_2SO_4 or $HClO_4$) even with high oxidant concentration (for chemical polymerization) or high anodic current, thus indicating that chlorination of mCIA is a prerequisite for polymerization. The same happens for feeds with high values of f_2 .
- 3) There was no evidence, in the experiments reported before [8], and in this work, that the Cl contents of the copolymers increased after the products remained for long times in the reaction medium.

The polymer films were also studied by cyclic voltammetry; typical voltammograms are shown in Fig. 2. For high f_1 feeds the shape is typical of PANI films. It is observed that there are important changes in the response as f_1 diminishes, specially for $f_1 < 0.5$, with an important decrease in the voltammetric charge; also, these films

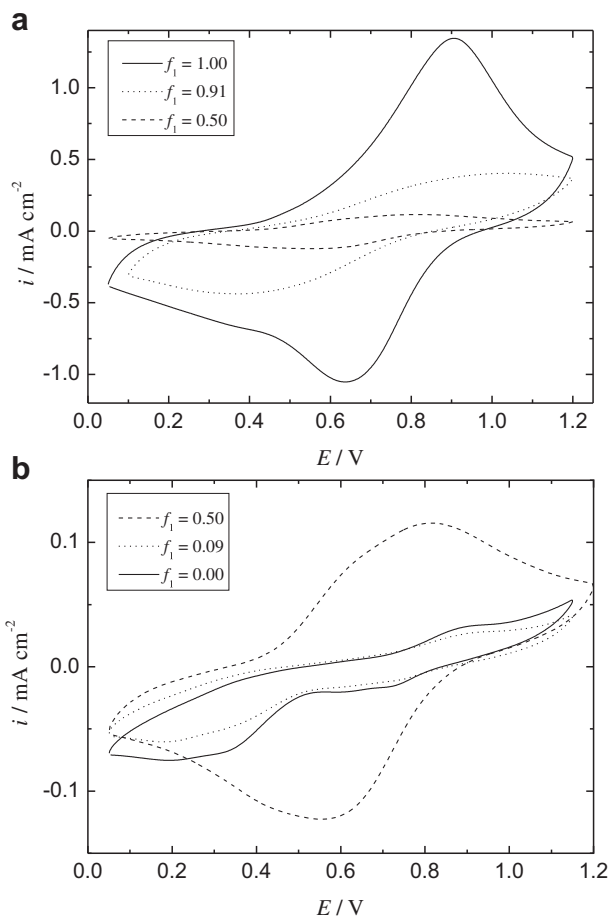


Fig. 2. Cyclic voltammograms of copolymer films for different mole fractions of aniline in the feed, f_1 . (a) $f_1 \geq 0.5$; (b) $f_1 \leq 0.5$. Notice the different scales. HCl 2 M, 50 mV s^{-1} .

show an orange-brownish color, different from the typical green color shown by films of PANI and copolymers with high Anisole contents. Also, for low anisole contents the voltammograms show a more resistive behavior.

3.2. Fluorescence measurements

Fig. 3 shows the fluorescence emission spectra (at different electrode potentials, E) of copolymers of different composition. The shape of these spectra has been previously discussed [5]. Briefly, the peaks observed at about 450 and 470 nm correspond to Raman dispersion, and are not related to polymer emission, which is the broad band below these peaks. This band decreases rather monotonically as the potential is increased; the decrease in the Raman peaks intensity comes from the changes in film absorbance. In Fig. 3a, where f_1 in the feed is low (0.17) there is almost no change in the fluorescence emission spectra with the electrode potential. In Fig. 3b ($f_1 = 0.83$) and c ($f_1 = 1.00$, pure PANI), a decrease in the fluorescence emission intensity is observed as the electrode potential is increased. Moreover, this decrease is more marked in the case of polyaniline (Fig. 3c).

The behavior observed in Fig. 3 clearly shows that the emission fluorescence spectra of copolymers with high mCIA content in the copolymerization feed is essentially not quenched as the electrode potential is increased. For copolymers with higher anisole content the emission is quenched with the increase in the electrode potential; this quenching is higher as the anisole content increases.

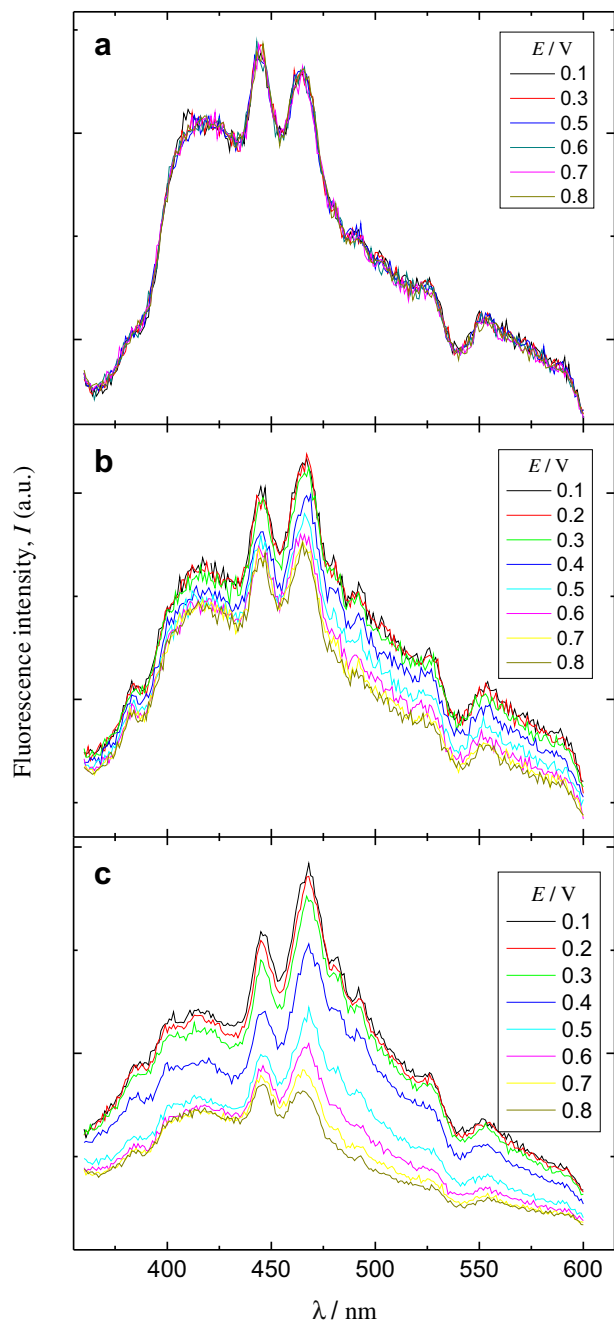


Fig. 3. Fluorescence emission spectra as a function of potential for different feed compositions. (a) $f_1 = 0.17$; (b) $f_1 = 0.83$; (c) $f_1 = 1.00$.

These results are in agreement with our previous work [8], where the spectroscopic properties of ANI-mCIA copolymers, obtained via a chemical synthesis, were studied in solution. In that work, it was observed, for the mCIA homopolymer and for copolymers with high mCIA content, that the emission and the relative fluorescence quantum yield were nearly constant, after the addition of a reducing agent.

To evaluate the fluorescence changes it should be considered the integrated (total) fluorescence emission I_{Tot} :

$$I_{\text{Tot}} = \int_{\lambda_{\text{min}}}^{\lambda_{\text{max}}} I(\lambda) d\lambda \quad (1)$$

where $I(\lambda)$ is the intensity at each wavelength and λ_{max} and λ_{min} are the spectrum limits. To achieve a correct comparison, the total intensities at each potential are normalized dividing by the largest one, which is that at the more cathodic potential, 0.1 V. Fig. 4 shows the relative fluorescence intensity, I_R :

$$I_R = \frac{I_{\text{Tot}}(E)}{I_{\text{Tot}}(0.1 \text{ V})} \quad (2)$$

as a function of the electrode potential, E , for different feed compositions. In general, the emission of fluorescence is affected by radiation absorption phenomena, thus appropriate corrections should in principle be applied [7]. However, it is verified that in Equation (2) these corrections essentially cancel out, thus they were omitted. Some features of Fig. 4 have been described previously [5,6,8]; considering the curve for the PANI homopolymer, it is seen that the fluorescence is quenched as the potential is increased, which is attributed to the introduction of quinone–imine units and thus additional energy levels as the polymer is gradually oxidized, causing quenching of the excited state. The electrode potential was not increased further to prevent polymer degradation, but even with higher potentials complete quenching is not achieved; this has been attributed to the morphology of PANI films, composed of crystalline conductive domains surrounded by amorphous regions (see Antonel et al. [6] and references therein): the conductive domains quench very efficiently the emission whereas the amorphous regions are less efficient, leaving a remaining emission, dependent on the film morphology. The introduction of chloroaniline monomers causes an increase of the emission at high potentials, that is, a decrease in quenching, which has been interpreted as due to the absence of quinone–imine units in dichloroaniline polymer segments [8]. It can be observed in Fig. 4 that as f_1 decreases the fluorescence quenching diminishes until that, for the dCIA homopolymer, there is no quenching. A striking feature is that for $f_1 = 0.999$, i.e., with only 0.1% mCIA in the feed there is already a marked change in the quenching behavior of the copolymer. In going from pure mCIA in the feed to increasing Ani contents, only for $f_1 = 0.9999$ ($f_2 = 10^{-4}$) the behavior of the PANI homopolymer is reached. Even without knowledge of the actual copolymer composition, this fact indicates that the introduction of a small proportion of chlorinated monomers disturbs significantly the polymer energy levels.

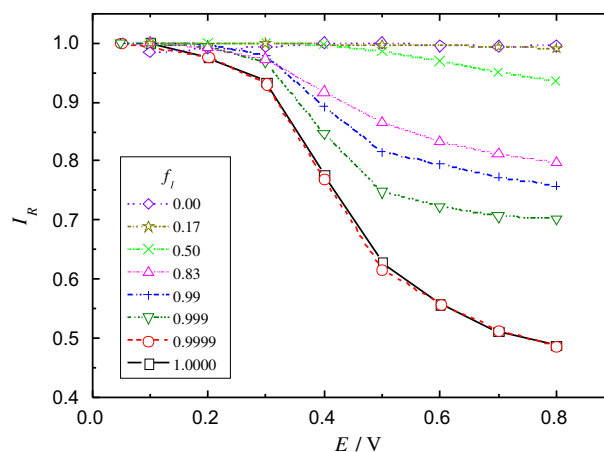


Fig. 4. Relative fluorescence quenching of copolymers as a function of applied potential for different feed compositions. The lines are a guide for the eyes.

4. Discussion

4.1. Terpolymerization mechanism

An interpretation of the fluorescence quenching under potential control requires consideration of the polymer microstructure. To that end, Monte Carlo simulations are performed in the framework of the terminal copolymerization model, requiring in turn kinetic parameters of the polymerization process; we thus begin analyzing the polymer composition as a function of feed composition.

The XPS measurement results of Fig. 1 show the incorporation of additional chlorine substituents in the polymer due to chlorination of the mCIA monomer to dCIA, as previously reported [8]. The fact that for $f_2 = 1.0$ it is found $F_{Cl} = 2.0$ (see Fig. 2) indicates that a dCIA homopolymer is formed, which in turn indicates that mCIA neither forms homopolymer nor copolymerizes with the dichlorinated monomer. On the other hand, the $F_{Cl}-f_1$ curve in the full composition range cannot be attributed to Ani-dCIA copolymerization without mCIA in the film; if that were the case, the system should follow the Mayo–Lewis equation [37]

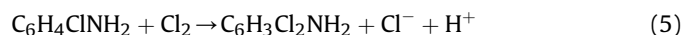
$$F_1 = \frac{r_1 f_1^2 + f_1 f_2}{r_1 f_1^2 + 2f_1 f_2 + r_2 f_2^2} \quad (3)$$

In Equation (3), the index 2 would correspond to dCIA units in the copolymer chain, and the Cl/N ratio would be simply $F_{Cl} = 2F_2$. The dotted line in Fig. 1 is the best fit found under such conditions (using the Levenberg–Marquardt algorithm, allowing both r_i parameters to vary simultaneously, resulting in $r_1 = 0.35$, $r_2 = 1.08$), which is clearly unsatisfactory. Additionally, Fig. S1 (Supplementary Information) compares the experimental data with curves calculated using Equation (3) for several pairs of reactivity ratio values, showing that the Mayo–Lewis equation does not describe adequately the experimental results. Thus, it is proposed that, in the general case, a terpolymerization between Ani, mCIA and dCIA takes place. It should be noted that mCIA monomers can indeed copolymerize with aniline, as observed by Li et al. [23] who worked with lower concentrations of HCl (1 M) and ammonium persulfate in a monomer:oxidant ratio of 1:0.5; in these conditions, mCIA–Ani copolymers were obtained, but mCIA in the absence of Ani did not polymerize, indicating that the conditions were not strong enough to produce chlorine and thus dichloroaniline. In our chemical polymerization study [8], stronger conditions were employed (2 M HCl, monomer:oxidant ratio 1:1), and a dichloroaniline polymer was obtained.

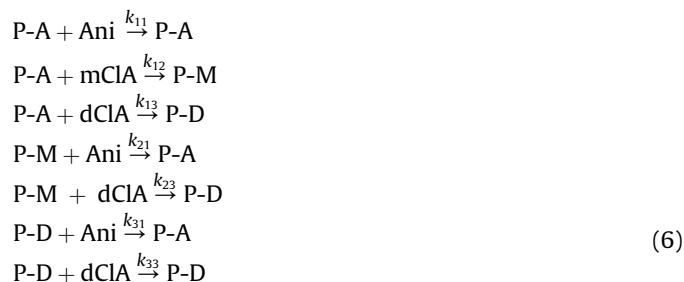
Next, we present a terpolymerization mechanism coupled to the mCIA chlorination reaction. As already discussed, chlorine is expected to evolve at the electrode:



The mCIA monomer is assumed to be chlorinated at the electrode surface, or at its immediate neighborhood:



The product of Equation (5), dichloroaniline, is expected to be mainly 2,3, 2,5 or 3,4 dichloro substituted; the last one will not polymerize due to the blocking of position 4; however the yield of this isomer should be lower due to the mechanism involving an N-chloro intermediate [38,39]. Other isomers, on the other hand, are able to copolymerize with Ani as previously reported [22]; here, we will refer to “dichloroaniline” in a general way, not making isomer distinction. Thus, the copolymer chains can propagate as follows:



where P-A, P-M and P-D represent electrode adsorbed intermediate chains ending in Ani, mCIA and dCIA monomers, respectively and k_{ij} are the rate constants; $i = 1, 2, 3$ correspond, respectively, to Ani, mCIA and dCIA. It should be borne in mind that, as it is well known [1], Equations (6) are coupled to oxidation of the polymer chains (reaction not shown) yielding 2e^- per monomer added. Based on the considerations above, reactions of addition of mCIA to chains ending in mCIA and dCIA have not been considered, i.e., rate constants k_{22} and k_{32} were assumed to be negligible. The following rate laws result:

$$\begin{aligned} R_{11} &= k_{11} \Gamma_1 c_1 \\ R_{12} &= k_{12} \Gamma_1 c_2 \\ R_{13} &= k_{13} \Gamma_1 c_3 \\ R_{21} &= k_{21} \Gamma_2 c_1 \\ R_{23} &= k_{23} \Gamma_2 c_3 \\ R_{31} &= k_{31} \Gamma_3 c_1 \\ R_{33} &= k_{33} \Gamma_3 c_3 \end{aligned} \quad (7)$$

Here, Γ_i is the surface concentration of chains ending in monomer i and c_i the respective monomer feed concentration. Furthermore, dCIA is formed in situ by Equation (5), with a rate assumed to be:

$$R_d = k_{2,d} [\text{Cl}_2] c_2 \quad (8)$$

Chlorine is formed electrochemically at the electrode (Equation (4)) and should partially leave the surface by gas evolution and mass transport. Here, as a simplifying assumption, mass transport of Cl_2 and dCIA will not be considered explicitly; because we are interested only in the stationary state, the concentration of these species should be stable. It is also assumed that the concentration of Cl_2 is constant through the experiments; this means that the rate of production and transport away from the electrode by diffusion and gas evolution is higher than the rate of consumption by Reaction (5). It should be kept in mind that the experiment is galvanostatic, thus the overall electrochemical reaction rate is forced to be constant; as shown in the following, that implies that the Cl_2 production rate is essentially constant throughout the experiment. At a constant current of 3 mA, the rate of Cl_2 production is about $10^{-8} \text{ mol cm}^{-2} \text{ s}^{-1}$ whereas the total amount of polymer formed at the end of the experiment (estimated from the voltammetric charge) is of the order of 10^{-9} – $10^{-8} \text{ mol cm}^{-2}$ monomer after 15 min of electropolymerization; oxygen evolution, on the other hand, should be negligible as its exchange current ($10^{-10} \text{ A cm}^{-2}$) is much lower than the chlorine evolution one ($10^{-3} \text{ A cm}^{-2}$). Thus, the presence of the polymer film does not preclude chlorine production, but causes a noticeable increase in the anodic potential: generally, it was about 2 V as soon as the current was applied, raising to ~ 2.2 V for Ani polymerization and over 3 V in the case of mCIA.

Based on the above considerations, Equation (8) will be written as

$$R_d = k_d c_2 \quad (9)$$

This implies that k_d is an apparent rate constant. The kinetic scheme of Equations (6) and (7) results, under stationary conditions, in the following system of differential equations [37,40,41]:

$$\begin{aligned} \frac{dN_1}{dt} &= R_{11} + R_{21} + R_{31} \\ \frac{dN_2}{dt} &= R_{12} \end{aligned} \quad (10)$$

$$\frac{dN_3}{dt} = R_{13} + R_{23} + R_{33}$$

with the steady state conditions:

$$\begin{aligned} \frac{dI_1}{dt} &= R_{21} - R_{12} + R_{31} - R_{13} = 0 \\ \frac{dI_2}{dt} &= R_{12} - R_{21} - R_{23} = 0 \\ \frac{dI_3}{dt} &= R_{13} - R_{31} + R_{23} = 0 \end{aligned} \quad (11)$$

where N_1 , N_2 and N_3 are the numbers of Ani, mCIA and dCIA monomers, respectively, in the growing polymer. Applying usual methods [40,41] the following relationships for copolymer composition are found:

$$\begin{aligned} \frac{dN_1}{c_1 \left(\frac{c_1}{r_{31}} + \frac{c_3}{r'r_{31}} \right) \left(c_1 + \frac{c_2}{r_{12}} + \frac{c_3}{r_{13}} \right)} &= \frac{dN_2}{c_1 \left(\frac{c_1}{r_{31}} + \frac{c_3}{r'r_{31}} \right) \frac{c_2}{r_{12}}} \\ &= \frac{dN_3}{c_3 \left(\frac{c_1}{r_{31}} + c_3 \right) \left(\frac{c_1}{r_{13}} + \frac{c_2}{r'r_{12}} + \frac{c_3}{r'r_{13}} \right)} \end{aligned} \quad (12)$$

where r_{12} , r_{13} and r_{31} are standard reactivity ratios given by $r_{ij} = k_{ij}/k_{ji}$, and $r' = k_{21}/k_{23}$ is the ratio of constants for the reactions of a chain ending in mCIA with Ani and dCIA [37].

Furthermore, as dCIA is produced in situ by Equation (5), we assume stationary state, given by:

$$\frac{dc_3}{dt} = R_d - R_{13} - R_{23} - R_{33} = 0 \quad (13)$$

Finally, as the polymerization proceeds on the electrode surface, it is assumed that the growing chains fully cover the surface, thus the following condition is assumed to hold:

$$\Gamma_1 + \Gamma_2 + \Gamma_3 = \Gamma_s \quad (14)$$

where Γ_s is the saturation surface concentration. Combining Equations (11), (13) and (14) the following condition for c_3 is found:

$$\frac{c_2}{r_d} \frac{c_3 \left(\frac{c_1}{r_{13}} + \frac{c_2}{r'r_{12}} + \frac{c_3}{r'r_{13}} \right) + \frac{c_1}{r''} \left(c_1 + \frac{c_2}{r''} + \frac{c_3}{r'} \right)}{c_3 \left(\frac{c_1}{r_{13}} + \frac{c_2}{r'r_{12}} + \frac{c_3}{r'r_{13}} \right)} - \frac{c_1}{r_{31}} - c_3 = 0 \quad (15)$$

Here, the constant ratios $r'' = k_{11}/k_{31}$ and $r''' = k_{21}/k_{12}$ are introduced as dimensionless parameters, as well as $r_d = k_{33} \Gamma_s/k_d$, which represents the ratio of consumption to production of dCIA in a medium initially containing only mCIA. Equation (15) allows, if c_1 , c_2 and the several r parameters are known, to compute the concentration of dCIA. It should be taken into account that, being obtained the polymer films by electropolymerization on an electrode surface, the amount of product is very small compared with the total monomer present, thus the degree of conversion is necessarily low. Also, because the gas evolution causes convection

in the electrode neighborhood, the monomer concentrations can be considered constant throughout the experiment. Thus, using Equation (12) the copolymer composition can be computed as the mole fraction of each monomer:

$$F_i = \frac{N_i}{\sum_{j=1}^3 N_j} \quad (16)$$

and the Cl/N ratio is thus given by

$$F_{Cl} = 2F_3 + F_2 \quad (17)$$

The model represented by Equations (12) and (15) can be fitted to the experimental data in order to obtain the kinetic parameters. However, there are in total seven adjustable parameters, too many for a reasonable confidence in the results; thus, some considerations are introduced to restrict the parameter range:

- 1) Díaz et al. [22] studied the copolymerization of aniline and three dichloroaniline isomers, obtaining the corresponding reactivity ratios; these ratios (named here as r_A and r_D for Ani and dCIA respectively) fall in the ranges 0.10–1.20 for r_A and 0.53–0.62 for r_D . They correspond, in the mechanism given in Equation (6), to r_{13} and r_{31} , respectively; thus these parameters were restricted to the ranges $0.05 \leq r_{13} \leq 1.25$ and $0.50 \leq r_{31} \leq 0.65$.
- 2) An initial estimate for r_{12} is obtained from the copolymer prepared with the lowest non zero f_2 : for $f_1 = 0.91$, $F_{Cl} = 0.20$; if it is assumed that for this case, being expected a relatively fast polymerization, chlorine in the copolymer will be mostly present in mCIA units, this can be treated with the Mayo–Lewis equation (Equation (3)) with $r_2 = 0$ (as mCIA does not homopolymerize) and $F_1 = 1 - F_{Cl}/2$, resulting in $r_1 \approx 0.29$; thus, r_{12} in the fitting was restricted to the range 0.2–0.4.
- 3) For a feed with mCIA alone ($c_1 = 0$), the steady state concentration of dCIA is given by $c_3 = c_2/r_d$; thus if r_d takes values below unity c_3 will be higher than c_2 . Even taking into account that this is the concentration in the electrode surface, which is expected to decay more or less rapidly toward the bulk value (which is 0 here), the lower limit for r_d was set to 1.5 to avoid excessively higher c_3 values.

The equation system (12), (15)–(17) was numerically solved with the aid of package Mathematica (Wolfram Research, Inc) using a Nelder–Mead algorithm [42] for global optimization, fitting F_{Cl} to the experimental results of Fig. 1. The solid line in Fig. 1 shows the fitted curve to the terpolymerization model, which is satisfactory. It was also verified that direct numerical integration of the rate equation system, Equations (10), (11) and (13), gave identical results. The resulting kinetic parameters were $r_{12} = 0.40$, $r_{13} = 0.05$, $r_{31} = 0.65$, $r_d = 1.5$, $r' = 0.20$, $r'' = 0.34$, $r''' = 10$. The three reactivity ratios, being below unity (and, besides, $k_{22} = 0$) indicate a tendency to alternate of the three monomers. Fig. S2 (Supplementary Information) shows the copolymer composition, the average chlorine atoms per unit, and the dCIA concentration, c_3 , predicted by the terpolymerization model.

4.2. Monte Carlo simulations

Kinetic simulations by the Monte Carlo method were performed to obtain sequence-length distributions for different feed compositions. The model stated in the previous section (Equations (7) and (9)) is employed, with the assumptions already made, and the additional assumption that the initiation and termination reactions are not considered explicitly; P-A is assumed to be present initially,

that is $\Gamma_1 = \Gamma_s$ because aniline is the most reactive monomer. Because only the steady state is studied (see below), this assumption has no influence on the results. The procedure involved the addition of M total monomers to n_C chains as follows:

- 1) For a given feed composition f_1 the monomer concentrations were set as $c_1 = f_1$, $c_2 = f_2$ and $c_3 = M_3/M$ where M_3 , the number of dCIA monomers, was initially zero.
- 2) Γ_s was arbitrarily set to n_C/M ; for $i = 1-3$, the surface coverage of chains ending in each monomer was set as $\Gamma_i = n_i/M$; initially, $n_1 = n_C$ and $n_2 = n_3 = 0$. The numbers of the three monomers in the copolymer, N_i , were all initially set to 0.
- 3) The rate constants were computed setting $k_{11} = 1$ and calculating the remaining from the set of r parameters found in the fitting.
- 4) In each simulation step, the reaction rates according to Equations (7) and (9) were computed and normalized to get the reaction probabilities, and one reaction was chosen at random based on these probabilities.
- 5) If reaction (9) was selected, M_3 was increased by one. In any other case, a monomer addition to a chain took place; a chain was chosen at random, the corresponding monomer was added to that chain and the values of the n_i and N_i were modified accordingly. If a dCIA monomer was added, M_3 was decreased by one.
- 6) The above procedure (1–5) was repeated until a steady state was reached, defined by constancy of M_3 and all the F_i .
- 7) Once the steady state was reached, the N_i were reset to 0, and the procedure given in 1–5 were repeated for a total of M steps, recording in an array the monomers added to each chain.
- 8) After finishing item 7), the arrays were analyzed to compute the sequence-length distribution as the number of segments, n_l for each length l , for both Ani and dCIA. In the case of mCIA obviously all segments have length l as $k_{22} = 0$. Also, the predicted copolymer fractions F_i (Equation (16)) were computed, as well as F_{CI} .

The above procedure was implemented in the FORTRAN programming language using a lagged Fibonacci random number generator [43] providing a long sequence and fast implementation. The number of monomers M were typically set to 4×10^7 ; it was verified that the results were independent of M for $M > 10^7$. For n_C , values between 100 and 40,000 give identical results; the value used was typically 1000, because higher values increased significantly the computation time. Only in the case of $f_1 = 0.999$ there were some noticeable fluctuations (due to the very low c_3) thus longer runs and averaging were employed. The open symbols in Fig. 1 show the Monte Carlo results for F_{CI} as a function of f_1 ; it is seen that they match the results obtained from the analytical model thus verifying the correctness of the procedure.

Fig. 5 shows the sequence length distributions predicted by Monte Carlo simulations; in Fig. 5a and b aniline sequences are shown; it is observed that for low aniline contents in the feed ($f_1 < 0.5$) only very short sequences of aniline monomers are present, with a high proportion of isolated aniline monomers. Fig. 5c shows the corresponding results for dCIA sequence lengths; it is observed a behavior similar to Ani, increasing the lengths as f_1 decreases, with a tendency to show shorter sequences than Ani. It was verified that different sets of kinetics parameters compatible with the copolymer composition shown in Fig. 1 lead to similar sequence-length distributions. The restrictions in the fitting procedure above lead to parameters with physically reasonable values. A less restricted fitting procedure yields other value sets for the r parameters, quite different from those reported in Section 4.1 and physically less reasonable, but also showing a good fitting; the sequence-length distributions deduced from Monte Carlo

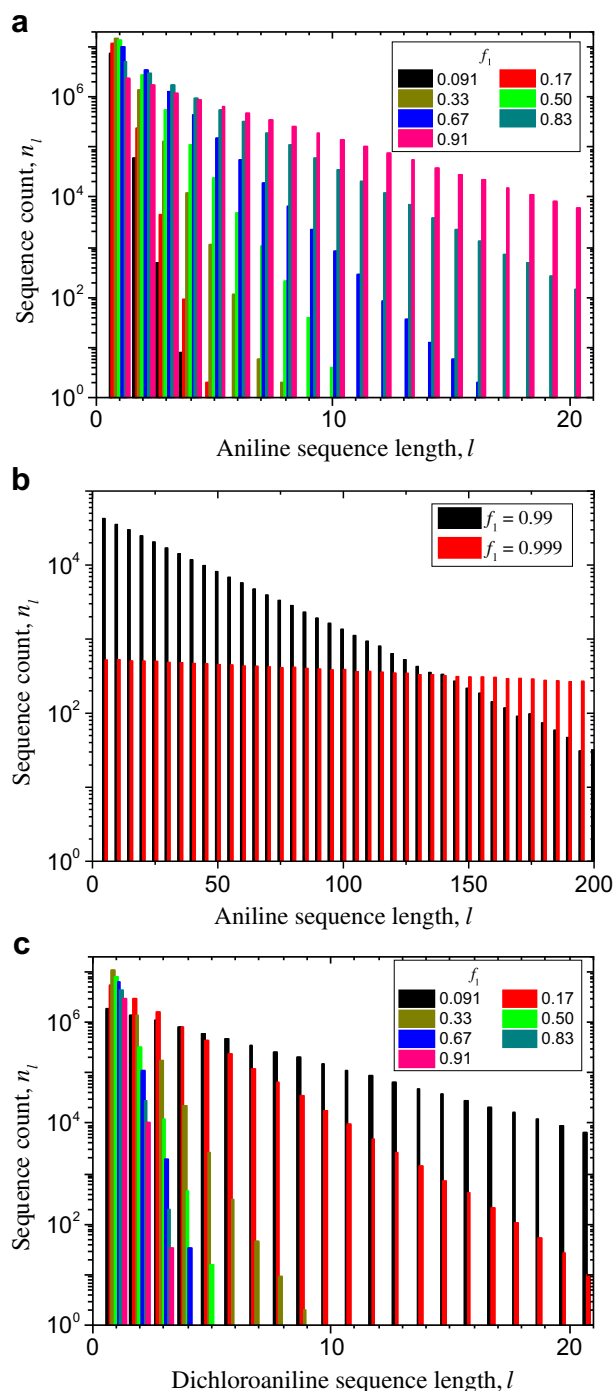


Fig. 5. Sequence length distributions predicted by Monte Carlo simulations for aniline (a and b) and dichloroaniline (c) sequences for different feed compositions.

simulations using these parameters are qualitatively very similar to those presented in Fig. 5.

To analyze the dependence of the fluorescence behavior with the polymer microstructure, we compare in Fig. 6 the quenching at the anodic limit, defined as:

$$\Delta I_{R,a} = I_R(0.1 \text{ V}) - I_R(0.8 \text{ V}) \quad (18)$$

with the total aniline monomer fraction in the polymer, F_1 , as well as $F_{1,j}$, the fraction of aniline monomers contained in sequences of length $l \geq j$, for $j = 2, 3$ and 4.

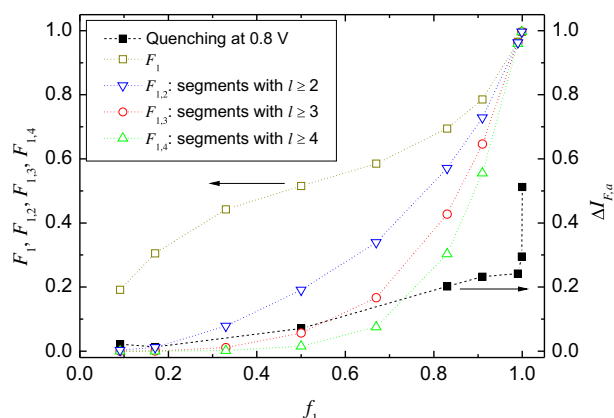


Fig. 6. Comparison of the fluorescence quenching at the anodic limit (closed symbols) with the total fraction of aniline monomers, and the fraction of aniline in sequences of length at least of 2, 3 and 4 segments (open symbols). The lines are a guide for the eyes.

It is already clear from the results shown in Fig. 4 that the presence of aniline monomers is necessary for the quenching of fluorescence. However, Fig. 6 shows that quenching does not correlate well with the total number of Anil monomers; instead, for low f_1 it follows closely the number of monomers found in segments of at least three aniline units. Three consecutive Anil monomers is the minimum needed to allow the formation of quinone–imine groups upon oxidation; poly(dichloroaniline) does not develop stable quinone–imine units, as shown in our previous study [8]. Thus, quenching should be the consequence, in this range of f_1 , of the presence of quinone–imine units, not necessarily of the electric conductance, which requires at least tetramers of aniline [44]; the increase in quenching thus follows the introduction, in a film of essentially poly(dichloroaniline), of sequences with 3 or more Anil units. For $f_1 > 0.6$, the fraction of Anil monomers in segments with $l \geq 3$ grows rapidly whereas quenching does not. However, for high values of f_1 inspection of Fig. 5c reveals that dCIA sequences are very short, mostly single units, and mCIA are always isolated units, thus in this conditions the film is essentially a PANI structure with isolated mono and dichloroaniline units inserted; the photophysical behavior should be, consequently, essentially that of PANI with some amount of chlorinated monomer units. On the other hand, when a few chloroaniline units are inserted in PANI there is a marked change in the fluorescence quenching: for $f_1 = 1.000$ about 51% of the emission is quenched, whereas for $f_1 = 0.999$ only $\sim 30\%$ change in intensity is observed; for this feed composition it is found from Equations (12) and (15) that $F_1 = 0.9962$, $F_2 = 2.5 \times 10^{-3}$ and $F_3 = 1.3 \times 10^{-3}$. Thus, the introduction of about 0.4% chloroaniline units causes a 40% decrease in quenching. A rough estimation from these numbers, assuming that the loss in quenching is equal to the number of Anil monomers involved, yields that one chloroaniline (either mono- or di-) affects about 100 Anil units. There are two possible explanations, not mutually exclusive, for this effect:

- 1) The most efficient quenching is expected to come from the crystalline conductive domains, where close lateral coupling between polymer chains allow electron delocalization [6,12,13,45]. The introduction of relatively bulky Cl substituents will disrupt the lateral coupling and consequently delocalization, eventually decreasing the size of such domains.
- 2) Besides lateral coupling, obviously delocalization along PANI chains due to conjugation is needed for efficient quenching. Because chloroanilines are not oxidized in the potential range

studied [8] its introduction will break the conjugation and hence prevent quenching.

The second consideration could not certainly explain the full effect on quenching, as it would require that a single mCIA or dCIA monomer disturbs the conjugation of about 100 units along the chain. Likely, its presence would affect a much shorter segment, which can be estimated of at least 4 units, as this a “redox” unit in PANI films and the minimum chain to achieve a noticeable conductivity [44]. However, in the crystalline domains there is a three-dimensional coupling leading to state delocalization, energy level separation of a few meV and, ultimately, efficient quenching [46,47]. According to Pouget et al. [10] emeraldine salt PANI synthesized in the presence of HCl forms closely packed pseudoorthorhombic crystalline domains with lattice parameters $a = 4.3 \text{ \AA}$, $b = 5.9 \text{ \AA}$ and $c = 9.6 \text{ \AA}$, the Cl^- ions filling the voids between chains. The introduction of one or two Cl substituents will certainly disturb the crystalline arrangement and interrupt the lateral coupling between chains. In the lattice, each chain has 8 nearest neighbors and 16 s-nearest neighbors; if the nearest, and some second-nearest neighbors are affected, with a minimum of 4 units in each chain, the ratio of 1 chloroaniline affecting roughly 100 Anil units can be explained. We thus attribute the marked decrease in quenching for $f_1 = 0.999$ to the combined effect of breaking the conjugation, in the oxidized state, in the chain where the chloroaniline monomer is located and the steric effect which either prevents or creates defects in the formation of crystalline domains responsible for efficient quenching.

4.3. Concluding remarks

Concluding, it has been found that the quenching of polyaniline fluorescence by polymer oxidation to the emeraldine state is affected by copolymerization with *m*-chloroaniline, with a strong decrease in the presence of 0.1% mCIA monomers in the feed, and is further diminished as mCIA feed contents increases. The presence of dichloroaniline units in the copolymer was confirmed and a terpolymerization reaction scheme where one of the monomers is produced in situ was introduced for the first time, obtaining the kinetic parameters. A Monte Carlo simulation of the terpolymerization model including the chlorination step was also introduced for the first time. The sequence length distributions for different compositions were obtained and compared, finding that quenching, for low aniline contents, is given by Anil sequences of at least three units. The strong decrease in quenching at low mCIA contents is attributed to a double effect: breaking of conjugation in the emeraldine form by the presence of the chlorinated unit, and a disruption of the close chain packing in the crystalline domains, preventing state delocalization and thus efficient quenching.

Acknowledgment

The authors gratefully acknowledge financial support for this research from de Universidad de Buenos Aires, the Consejo Nacional de Investigaciones Científicas y Técnicas (CONICET, Argentina) and the Agencia Nacional de Promoción Científica y Tecnológica, Argentina. P.S.A. and F.V.M are members of the Carrera del Investigador Científico of CONICET.

Appendix A. Supplementary data

Supplementary data related to this article can be found online at doi:10.1016/j.polymer.2012.04.041.

References

- [1] Chandrasekhar P. Conducting polymers, fundamentals and applications: a practical approach. 1st ed. New York: Springer; 1999.
- [2] Skotheim TA, Reynolds J, editors. Conjugated polymers: processing and applications. 3rd ed. Boca Raton, FL, USA: CRC Press; 2006.
- [3] Son Y, Patterson HH, Carlin CM. Chem Phys Lett 1989;162:461–6.
- [4] Ram MK, Mascetti G, Paddeu S, Maccioni E, Nicolini C. Synth Met 1997;89:63–9.
- [5] Antonel PS, Andrade EM, Molina FV. Electrochim Acta 2004;49:3687–92.
- [6] Antonel PS, Molina FV, Andrade EM. J Electroanal Chem 2007;599:52–8.
- [7] Antonel PS, Andrade EM, Molina FV. J Electroanal Chem 2009;632:72–9.
- [8] Antonel PS, Andrade EM, Molina FV. React Funct Polym 2009;69:197–205.
- [9] Pickup PG. In: White RE, Bockris JO, Conway BE, editors. Modern aspects of electrochemistry, number 33. 1st ed. New York: Springer; 1999. p. 307–434.
- [10] Pouget JP, Jozefowicz ME, Epstein AJ, Tang X, MacDiarmid AG. Macromolecules 1991;24:779–89.
- [11] Joo J, Oblakowski Z, Du G, Pouget JP, Oh EJ, Wiesinger JM, et al. Phys Rev B 1994;49:2977–80.
- [12] Wu C-G, Chang S-S. J Phys Chem B 2004;109:825–32.
- [13] Krinichnyi VI, Tokarev SV, Roth H-K, Schrodner M, Wessling B. Synth Met 2005;152:165–8.
- [14] Wei Y, Hariharan R, Patel SA. Macromolecules 1990;23:758–64.
- [15] Li X-G, Huang M-R, Zhu L-H, Yang Y. J Appl Polym Sci 2001;82:790–8.
- [16] Motheo AJ, Pantoja MF, Venancio EC. Solid State Ionics 2004;171:91–8.
- [17] Li X, Zhou H, Huang M. J Polym Sci A Polym Chem 2004;42:6109–24.
- [18] Li XG, Zhou HJ, Huang MR. Polymer 2005;46:1523–33.
- [19] Kim EM, Jung CK, Choi EY, Gao C, Kim SW, Lee SH, et al. Polymer 2011;52:4451–5.
- [20] Sasikumar R, Manisankar P. Polymer 2011;52:3710–6.
- [21] Shah A-HA, Bilal S, Holze R. Synth Met 2012;162:356–63.
- [22] Díaz F, Sánchez C, del Valle M, Torres J, Tagle L. Synth Met 2001;118:25–31.
- [23] Li X-G, Huang M-R, Lu Y-Q, Zhu M-F. J Mater Chem 2005;15:1343.
- [24] Waware US, Umare SS. React Funct Polym 2005;65:343–50.
- [25] Binder K. Monte Carlo and molecular dynamics simulations in polymer science. Oxford University Press; 1995.
- [26] Platkowski K, Reichert K-H. Polymer 1999;40:1057–66.
- [27] Feng J, Ruckenstein E. Polymer 2002;43:5775–90.
- [28] Termonia Y. Polymer 2009;50:1062–6.
- [29] Sun D, Guo H. Polymer 2011;52:5922–32.
- [30] Tobita H. Macromolecules 1993;26:836–41.
- [31] Zaldivar D, Fuentes G, Monett D, Peniche C, Arcis RW, Soto A, et al. Lat Am Appl Res 2002;32:117–22.
- [32] Anantawaraskul S, Soares JBP, Wood-Adams PM. Macromol Theor Simul 2003;12:229–36.
- [33] Hou C, Sun C, Ying L, Wang C. J Appl Polym Sci 2005;96:483–8.
- [34] Mohammadi Y, Najafi M, Haddadi-Asl V. Macromol Theor Simul 2005;14:325–36.
- [35] Athawale (née Bedekar) AA, Patil SF, Deore B, Patil RC, Vijayamohan K. Polym J 1997;29:787–94.
- [36] Morales GM, Llusa M, Miras MC, Barbero C. Polymer 1997;38:5247–50.
- [37] Mayo FR, Walling C. Chem Rev 1950;46:191–287.
- [38] Haberfield P, Paul D. J Am Chem Soc 1965;87:5502.
- [39] Gassman PG, Campbell GA. J Am Chem Soc 1971;93:2567–9.
- [40] Alfrey T, Goldfinger G. J Chem Phys 1944;12:322.
- [41] Walling C, Briggs ER. J Am Chem Soc 1945;67:1774–8.
- [42] Nelder JA, Mead R. Comput J 1965;7:308–13.
- [43] Petersen W. Int J High Speed Comp 1994;6:387–98.
- [44] Surwade SP, Manohar N, Manohar SK. Macromolecules 2009;42:1792–5.
- [45] Prigodin VN, Epstein AJ. Europhys Lett 2002;60:750–6.
- [46] Prigodin VN, Epstein AJ. Synth Met 2001;125:43–53.
- [47] Sutar DS, Tewari R, Dey GK, Gupta SK, Yakhmi JV. Synth Met 2009;159:1067–71.